Journal of Sound and Vibration 327 (2009) 424–439

Contents lists available at ScienceDirect

Journal of Sound and Vibration

journal homepage: www.elsevier.com/locate/jsvi

On the similarity of the Coleman and Lyapunov–Floquet transformations for modal analysis of bladed rotor structures

P.F. Skjoldan [a,*], M.H. Hansen [b]

[a] Loads, Aerodynamics and Control, Siemens Wind Power A/S, Dybendalsvænget 3, DK-2630 Taastrup, Denmark
[b] National Laboratory for Sustainable Energy, Risø – Technical University of Denmark, Frederiksborgvej 399, DK-4000 Roskilde, Denmark

ARTICLE INFO

Article history:
Received 4 December 2008
Received in revised form
27 May 2009
Accepted 13 July 2009
Handling Editor: M.P. Cartmell
Available online 14 August 2009

ABSTRACT

Structures with isotropic bladed rotors can be modally analyzed by eigenvalue analysis of time-invariant Coleman transformed equations of motion related to the inertial frame or by Floquet analysis of the periodic equations of motion. The Coleman transformation is here shown to be a special case of the Lyapunov–Floquet (L–F) transformation which transforms system equations of structures with anisotropic bladed rotors into a time-invariant system using the transition matrix and Floquet eigenvectors as a basis. The L–F transformation is not unique, whereby eigensolutions of the time-invariant system are not directly related to the modal frequencies and mode shapes observed in the inertial frame. This modal frequency indeterminacy is resolved by requiring the periodic mode shapes from the L–F approach to be as similar as possible to the mode shapes from the Coleman approach. For an anisotropic rotor the Floquet analysis yields a periodic mode shape that contains harmonics of integer multiples of the rotor speed for inertial state variables. These harmonic components show up as resonance frequencies on the sides of the corresponding modal frequency in a computed frequency response function of a simple three-bladed turbine with an anisotropic rotor.

1. Introduction

The Coleman and Lyapunov–Floquet (L–F) transformations can be used to obtain time-invariant system equations for modal and stability analysis of structures with bladed rotors, e.g. wind turbines and helicopters. This paper explores a similarity of these transformations and uses the physical basis of the Coleman transformation to resolve the indeterminacy of the modal frequencies in Floquet analysis due to the non-uniqueness of the L–F transformation.

Coleman [1] introduces a transformation of the coordinates of bladed rotors into multi-blade coordinates describing the rotor motion in the inertial frame of reference. The periodic coefficients can thereby be eliminated in the system equations for isotropic rotors, where the blades are identical and symmetrically mounted. Feingold [2] extends the work by Coleman to show that the periodic coefficients can also be eliminated in the equations of inplane motion for two-bladed rotors if the rotor support is symmetric. Coleman and Feingold [3] show that for two-bladed rotors with an asymmetric support, the Coleman transformation yields system equations containing periodic terms that have a frequency of two times the rotor speed. They use Floquet theory [4] to show that the solution to a linear periodic system can be written as a set of exponential functions containing the characteristic exponents (each representing a frequency and damping) multiplied by a corresponding set of periodic functions that contain harmonics with integer multiples of the system frequency. Any

* Corresponding author. Tel.: +45 44774865.
E-mail address: peter.skjoldan@siemens.com (P.F. Skjoldan).

0022-460X/$ - see front matter © 2009 Elsevier Ltd. All rights reserved.
doi:10.1016/j.jsv.2009.07.007

periodic function can be represented by a Fourier series, which is used in Hill's method to derive the characteristic exponents from Hill's determinant (see, e.g. [5–7]) as Coleman and Feingold do in their stability analysis of two-bladed rotors.

The development of digital numerical analysis allows direct application of Floquet theory by computation of the transition matrix from the time integration of the system equations. The transition matrix gives the *monodromy matrix* whose eigenvalues are the Floquet multipliers that determine the characteristic exponents with non-unique frequencies. Early Floquet analyses are performed on helicopters by Lowis [8] using a rectangular ripple method and Peters and Hohenemser [9] using a predictor–corrector integration scheme. Attempts to reduce the immense computational effort required by Floquet analysis on larger systems are done by Friedmann et al. [10] who develop an efficient numerical scheme to obtain the transition matrix from a single integration, and by Sinha and Pandiyan [11] who approximate the transition matrix based on an expansion of the system matrix in Chebyshev polynomials. Peters [12] shows with *fast Floquet theory* that the transition matrix computed until $1/B$ of the system period for an isotropic rotor with B blades can be used to generate the transition matrix for the full period. Bauchau and Nikishkov [13] use elements of the Arnoldi eigenvalue algorithm to perform *implicit Floquet analysis* yielding the most important eigensolutions from a limited number of system matrix integrations. Concepts of system identification from experimental signal analysis are applied by Quaranta et al. [14] to project the state variables of a large multi-body dynamical system by proper orthogonal decomposition into a smaller subspace before applying Floquet analysis. Bauchau and Wang [15] use a similar approach, *partial Floquet analysis*, to approximate the monodromy matrix from an incomplete transition matrix.

The modal frequencies and damping of the vibration modes of the periodic system can be determined from the Floquet multipliers. The infinity of solution branches to the complex logarithm yields frequencies given by a principal value plus an integer multiple of the system frequency. The traditional approach for resolving this frequency indeterminacy is based on Fourier analysis of the set of periodic functions in the Floquet solution [16,17], which are herein referred to as the *periodic mode shapes*. This method is contained in several different Floquet approaches [15,18,19]. Nagabhushanam and Gaonkar [20] suggest an automatic modal identification method, where the integer factor of the frequency indeterminacy is determined by using that the ratio of the velocity and position parts of the dominating degree of freedom in the Floquet eigenvectors is an estimate of the modal frequency. Peters and Hohenemser [9] increase the magnitude of the system periodicity in small increments starting from zero, where the frequencies are unique, until the desired value, and thus obtain the modal frequencies by continuation.

In this paper, the traditional method for resolving the frequency indeterminacy is substantiated by showing a similarity between the modal dynamics of an isotropic rotor obtained by eigenvalue analysis of the Coleman transformed system equations and the modal dynamics obtained by Floquet analysis. The comparison is based on *Lyapunov's reducibility theorem* [21] stating that the periodic Lyapunov–Floquet (L–F) transformation eliminates the periodic coefficients in the system equations. The L–F transformation is not unique, because it depends on the non-unique characteristic exponents. The choice of integer factors on the rotor speed added to the characteristic exponents can be considered as a choice of reference frame into which the state variables are L–F transformed, and in which the frequencies are then measured. Modal frequencies are herein defined to be measured in the inertial frame, whereby they can be directly compared to the modal frequencies obtained from the eigenvalues of the Coleman transformed system equations. The inertial state variables in the periodic mode shape obtained from the Coleman transformed equations are constant; therefore the modal frequencies are chosen such that the harmonic components of the inertial state variables in the periodic mode shape become as constant as possible. In the comparison of the two approaches for an isotropic rotor, the same results are obtained. This frequency identification approach in Floquet analysis is, however, applicable to a system with anisotropic rotor and support.

The paper is arranged as follows: Section 2 contains the theory of modal analysis using the Coleman transformation and using Floquet analysis. The similarity of the two approaches is shown and used as a basis for resolving the frequency indeterminacy. Section 3 contains a numerical example that compares the two approaches for an isotropic rotor and uses Floquet analysis for an anisotropic rotor. Section 4 contains the conclusions.

2. Modal analysis of structures with bladed rotors

The linear equations of motion for small vibrations of a structure with a bladed rotor operating at constant mean rotor speed with small overlaid variations can be written as a set of first-order equations:

$$\dot{\mathbf{x}} = \mathbf{A}(t)\mathbf{x}, \quad \mathbf{A}(t+T) = \mathbf{A}(t) \tag{1}$$

where $(\dot{})$ denotes the time derivative, $\mathbf{A}$ is the periodic system matrix, $T = 2\pi/\Omega$ is the period corresponding to the mean rotor speed Ω, and $\mathbf{x}$ is the state vector for a rotor with B blades:

$$\mathbf{x} = \{x_{1,1} \cdots x_{1,N_\mathrm{b}} \;\; x_{2,1} \cdots x_{2,N_\mathrm{b}} \;\; \cdots \;\; x_{B,1} \cdots x_{B,N_\mathrm{b}} \;\; x_{\mathrm{s},1} \cdots x_{\mathrm{s},N_\mathrm{s}}\}^\mathrm{T} \tag{2}$$

where an integer as the first index on x denotes the blade number and "s" as the first index denotes *inertial state variables* of the rotor support. The total number of state variables for a B-bladed rotor system is $N = BN_\mathrm{b} + N_\mathrm{s}$, where N_b is the number of *rotor state variables* in the rotating frame for a single blade and N_s is the number of inertial state variables of the rotor support. It is assumed that all blades have identical sets of state variables. Note that the state variables for an

aeroservoelastic model of a wind turbine or helicopter may consist of generalized coordinates and velocities of structural motion, state variables of the unsteady aerodynamic model, and state variables of the controller.

2.1. Coleman transformation approach

The Coleman transformation for a rotor with B blades is [12,16]

$$\mathbf{x} = \mathbf{B}(t)\mathbf{z}_{\mathrm{B}}$$

$$\mathbf{B}(t) = \begin{bmatrix} \mathbf{I}_{N_\mathrm{b}} & \mathbf{I}_{N_\mathrm{b}}\cos\psi_1 & \mathbf{I}_{N_\mathrm{b}}\sin\psi_1 & \cdots & \mathbf{I}_{N_\mathrm{b}}\cos\tilde{B}\psi_1 & \mathbf{I}_{N_\mathrm{b}}\sin\tilde{B}\psi_1 & -\mathbf{I}_{N_\mathrm{b}} & \mathbf{0} \\ \mathbf{I}_{N_\mathrm{b}} & \mathbf{I}_{N_\mathrm{b}}\cos\psi_2 & \mathbf{I}_{N_\mathrm{b}}\sin\psi_2 & \cdots & \mathbf{I}_{N_\mathrm{b}}\cos\tilde{B}\psi_2 & \mathbf{I}_{N_\mathrm{b}}\sin\tilde{B}\psi_2 & \mathbf{I}_{N_\mathrm{b}} & \mathbf{0} \\ \mathbf{I}_{N_\mathrm{b}} & \mathbf{I}_{N_\mathrm{b}}\cos\psi_3 & \mathbf{I}_{N_\mathrm{b}}\sin\psi_3 & \cdots & \mathbf{I}_{N_\mathrm{b}}\cos\tilde{B}\psi_3 & \mathbf{I}_{N_\mathrm{b}}\sin\tilde{B}\psi_3 & -\mathbf{I}_{N_\mathrm{b}} & \mathbf{0} \\ \vdots & \vdots & \vdots & & \vdots & \vdots & \vdots & \vdots \\ \mathbf{I}_{N_\mathrm{b}} & \mathbf{I}_{N_\mathrm{b}}\cos\psi_B & \mathbf{I}_{N_\mathrm{b}}\sin\psi_B & \cdots & \mathbf{I}_{N_\mathrm{b}}\cos\tilde{B}\psi_B & \mathbf{I}_{N_\mathrm{b}}\sin\tilde{B}\psi_B & (-\mathbf{I}_{N_\mathrm{b}})^B & \mathbf{0} \\ \mathbf{0} & \mathbf{0} & \mathbf{0} & \cdots & \mathbf{0} & \mathbf{0} & \mathbf{0} & \mathbf{I}_{N_\mathrm{s}} \end{bmatrix} \tag{3}$$

where $\tilde{B} = (B-1)/2$ for B odd and $\tilde{B} = (B-2)/2$ for B even, $\psi_j = \Omega t + 2\pi(j-1)/B$ is the mean azimuth angle to blade number $j = 1, 2, \ldots, B$, and $\mathbf{I}_{N_\mathrm{b}}$ and $\mathbf{I}_{N_\mathrm{s}}$ are identity matrices of sizes N_b and N_s. The vector $\mathbf{z}_\mathrm{B}$ contains the BN_b state variables in multi-blade coordinates and N_s inertial state variables as

$$\mathbf{z}_\mathrm{B} = \{a_{0,1}\cdots a_{0,N_\mathrm{b}}\ a_{1,1}\cdots a_{1,N_\mathrm{b}}\ b_{1,1}\cdots b_{1,N_\mathrm{b}}\ \cdots\ a_{\tilde{B},1}\cdots a_{\tilde{B},N_\mathrm{b}}\ b_{\tilde{B},1}\cdots b_{\tilde{B},N_\mathrm{b}}\ b_{B/2,1}\cdots b_{B/2,N_\mathrm{b}}\ x_{\mathrm{s},1}\cdots x_{\mathrm{s},N_\mathrm{s}}\}^\mathrm{T} \tag{4}$$

and describes the rotor motion in the inertial frame. The second last column block in $\mathbf{B}$ and coordinates $b_{B/2,1}$ to $b_{B/2,N_\mathrm{b}}$ occur only for B even. Details on how multi-blade coordinates describe the motion of a three-bladed wind turbine rotor in the inertial frame are discussed in [22,23].

Insertion of (3) into (1) shows that the Coleman transformed system equation becomes

$$\dot{\mathbf{z}}_\mathrm{B} = \mathbf{A}_\mathrm{B}\mathbf{z}_\mathrm{B} \tag{5}$$

where

$$\mathbf{A}_\mathrm{B} = \mathbf{B}^{-1}(t)\mathbf{A}(t)\mathbf{B}(t) - \mathbf{B}^{-1}(t)\dot{\mathbf{B}}(t) \tag{6}$$

The transformed system matrix $\mathbf{A}_\mathrm{B}$ will be time-invariant if the rotor is *isotropic*, i.e. it has three or more blades with equal properties and has symmetric inter-blade couplings such that the coupling to the support depends only on the azimuth angle and not the blade number, as shown in Appendix A. This important feature of the Coleman transformation enables the use of traditional eigenvalue analysis for the modal decomposition of the dynamics of these particular rotors.

2.1.1. Modal decomposition of transient solution

A transient solution of the time-invariant Coleman transformed system equation (5) for an isotropic rotor with a constant system matrix $\mathbf{A}_\mathrm{B}$ is

$$\mathbf{z}_\mathrm{B} = \mathrm{e}^{\mathbf{A}_\mathrm{B}t}\mathbf{z}_\mathrm{B}(0) \tag{7}$$

where $\mathbf{z}_\mathrm{B}(0) = \mathbf{B}^{-1}(0)\mathbf{x}(0)$ are the inverse transformed initial conditions (i.e. the disturbance of the structure away from its operating point). The Coleman transformed system matrix can be written in terms of its Jordan form as $\mathbf{A}_\mathrm{B} = \mathbf{V}_\mathrm{B}\mathbf{\Lambda}_\mathrm{B}\mathbf{V}_\mathrm{B}^{-1}$ whereby the transient solution (7) becomes

$$\mathbf{z}_\mathrm{B} = \mathbf{V}_\mathrm{B}\,\mathrm{e}^{\mathbf{\Lambda}_\mathrm{B}t}\mathbf{V}_\mathrm{B}^{-1}\mathbf{z}_\mathrm{B}(0) \tag{8}$$

If the eigenvectors $\mathbf{v}_{B,k}$ of $\mathbf{A}_\mathrm{B}$ are all linearly independent, $\mathbf{\Lambda}_\mathrm{B}$ is a diagonal matrix containing the eigenvalues $\lambda_{B,k}$ of $\mathbf{A}_\mathrm{B}$, and the eigenvectors $\mathbf{v}_{B,k}$ form the columns of $\mathbf{V}_\mathrm{B}$ (see [24] for the case of repeated eigenvalues with linearly dependent eigenvectors).

The transient solution (8) can be transformed into the original coordinates by (3) as

$$\mathbf{x} = \mathbf{U}_\mathrm{B}(t)\,\mathrm{e}^{\mathbf{\Lambda}_\mathrm{B}t}\mathbf{q}_\mathrm{B}(0) \tag{9}$$

where

$$\mathbf{q}_\mathrm{B}(0) = \mathbf{V}_\mathrm{B}^{-1}\mathbf{B}^{-1}(0)\mathbf{x}(0) \tag{10}$$

is a constant vector representing the modal content of the initial conditions $\mathbf{x}(0)$, and

$$\mathbf{U}_\mathrm{B}(t) = \mathbf{B}(t)\mathbf{V}_\mathrm{B} \tag{11}$$

is a periodic mode shape matrix. This modal interpretation becomes clearer if the Jordan form $\mathbf{\Lambda}_B$ is diagonal, whereby (9) can be decomposed as

$$\mathbf{x} = \sum_{k=1}^{N} \mathbf{u}_{B,k}(t)\, e^{\lambda_{B,k} t} q_{B,k}(0) \tag{12}$$

where $\mathbf{u}_{B,k}(t) = \mathbf{B}(t)\mathbf{v}_{B,k}$ is a periodic mode shape of mode number k in the original coordinates. It can be shown by expanding (12) for state variable number i on blade number j that the rotor state variables can contain B different harmonic components (see [23] for details on a three-bladed rotor) written as

$$\begin{aligned} x_{ik} = e^{\sigma_{B,k} t} \Bigg(& A_{0,ik} \cos(\omega_{B,k} t + \varphi_{0,ik}) + \sum_{n=1}^{\tilde{B}} \Bigg(A_{\mathrm{BW}n,ik} \cos\Bigg((\omega_{B,k} + n\Omega) t + \frac{2\pi n}{B}(j-1) + \phi_{\mathrm{BW}n,ik} \Bigg) \\ & + A_{\mathrm{FW}n,ik} \cos\Bigg((\omega_{B,k} - n\Omega) t - \frac{2\pi n}{B}(j-1) + \phi_{\mathrm{FW}n,ik} \Bigg) \Bigg) + A_{B/2,ik} \cos(\omega_{B,k} t + \phi_{B/2,ik}) \Bigg) q_{B,k}(0) \end{aligned} \tag{13}$$

where $\sigma_{B,k}$ and $\omega_{B,k}$ are the modal damping and frequency, respectively, given by the eigenvalue $\lambda_{B,k} = \sigma_{B,k} + \mathrm{i}\omega_{B,k}$ with $\mathrm{i} = \sqrt{-1}$. The amplitudes are determined from the components of the eigenvector $\mathbf{v}_{B,k}$ in multi-blade coordinates (4) as $A_{0,ik} = |a_{0,ik}|$, $A_{B/2,ik} = |b_{B/2,ik}|$ (for B even only) and

$$\begin{aligned} A_{\mathrm{BW}n,ik} &= \tfrac{1}{2}\sqrt{(\mathrm{Re}(a_{n,ik}) + \mathrm{Im}(b_{n,ik}))^2 + (\mathrm{Re}(b_{n,ik}) - \mathrm{Im}(a_{n,ik}))^2} \\ A_{\mathrm{FW}n,ik} &= \tfrac{1}{2}\sqrt{(\mathrm{Re}(a_{n,ik}) - \mathrm{Im}(b_{n,ik}))^2 + (\mathrm{Re}(b_{n,ik}) + \mathrm{Im}(a_{n,ik}))^2} \end{aligned} \tag{14}$$

where $a_{n,ik}$ and $b_{n,ik}$ are the cosine and sine components of $\mathbf{v}_{B,k}$, respectively. The constant phases $\phi_{0,ik}$, $\phi_{\mathrm{BW}n,ik}$, $\phi_{\mathrm{FW}n,ik}$, and $\phi_{B/2,ik}$ in (13) are also given by the eigenvector [23]. The amplitudes with subscript BW denote the backward whirling components, where for $n = 1$ the reaction force due to this rotor motion rotates against the direction of the rotor. Conversely, the FW amplitudes represent the forward whirling components, where for $n = 1$ the reaction force rotates in the direction of rotor rotation. For $n > 1$ the reaction forces cancel out and these components are called reactionless.

2.2. Lyapunov–Floquet transformation approach

Floquet theory enables the solution of the linear equation system (1) directly without elimination of the periodic coefficients. Any transient solution at any time t can be formed from N linearly independent solutions of (1) over a single period $t \in [0; T]$ [6]. These solutions $\boldsymbol{\varphi}_k(t)$ are collected in the columns of an $N \times N$ matrix called the *fundamental matrix* of the system:

$$\boldsymbol{\varphi}(t) = [\boldsymbol{\varphi}_1(t)\ \ \boldsymbol{\varphi}_2(t)\ \ \cdots\ \ \boldsymbol{\varphi}_N(t)], \quad \dot{\boldsymbol{\varphi}}(t) = \mathbf{A}(t)\boldsymbol{\varphi}(t) \tag{15}$$

The solutions may be found by numerical solution of (1) with N linearly independent initial conditions collected as columns in the matrix $\boldsymbol{\varphi}(0)$. Lyapunov's reducibility theorem [25] states that there exists a transformation of the original coordinates $\mathbf{x}$ that renders the periodic system (1) time-invariant. This Lyapunov–Floquet transformation can be defined as [26,11,27]

$$\mathbf{x} = \mathbf{L}(t)\mathbf{z}, \quad \mathbf{L}(t) = \boldsymbol{\varphi}(t)\, e^{-\mathbf{R}t} \boldsymbol{\varphi}^{-1}(0)\mathbf{L}(0) \tag{16}$$

where $\mathbf{R}$ is a constant non-singular matrix.

To show that the Lyapunov–Floquet transformation (16) eliminates the periodic terms of the system equations, it is substituted into (1) leading to

$$\dot{\mathbf{z}} = \mathbf{L}^{-1}(t)(\mathbf{A}(t)\mathbf{L}(t) - \dot{\mathbf{L}}(t))\mathbf{z} \tag{17}$$

which by differentiation of $\mathbf{L}$ and use of $\dot{\boldsymbol{\varphi}}(t) = \mathbf{A}(t)\boldsymbol{\varphi}(t)$ can be rewritten as

$$\dot{\mathbf{z}} = \mathbf{A}_{\mathrm{L}}\mathbf{z} \tag{18}$$

where

$$\mathbf{A}_{\mathrm{L}} = \mathbf{L}^{-1}(0)\boldsymbol{\varphi}(0)\mathbf{R}\boldsymbol{\varphi}^{-1}(0)\mathbf{L}(0) \tag{19}$$

is the time-invariant Lyapunov–Floquet transformed system matrix. Note that it is given by the constant matrix $\mathbf{R}$, and the choices of initial conditions for the fundamental matrix $\boldsymbol{\varphi}(0)$ and transformation matrix $\mathbf{L}(0)$.

If the constant matrix $\mathbf{R}$ is defined in terms of the *monodromy matrix*

$$\mathbf{C} \equiv \boldsymbol{\varphi}^{-1}(t)\boldsymbol{\varphi}(t+T) \tag{20}$$

as

$$\mathbf{C} = e^{\mathbf{R}T} \tag{21}$$

then the Lyapunov–Floquet transformation $\mathbf{L}$ can be shown to be periodic with period T by combining (16), (20), (21), and $\mathbf{R} = \mathbf{V}\boldsymbol{\Lambda}\mathbf{V}^{-1}$.

The monodromy matrix can be written in terms of its Jordan form $\mathbf{C} = \mathbf{P}\mathbf{J}\mathbf{P}^{-1}$ where $\mathbf{J}$ contains the eigenvalues ρ_k of $\mathbf{C}$ in the diagonal. The eigenvalues are named *characteristic* or *Floquet multipliers*. Eq. (21) shows that $\mathbf{R}$ is determined as the matrix logarithm

$$\mathbf{R} = \frac{1}{T}\ln(\mathbf{C}) = \frac{1}{T}\mathbf{P}\ln(\mathbf{J})\mathbf{P}^{-1} \tag{22}$$

which exists because $\mathbf{C}$ is non-singular [28]; however, $\mathbf{R}$ may not be unique. There can be two causes of non-uniqueness of the matrix logarithm [29]: first, the similarity transformation matrix $\mathbf{V}$ of the Jordan decomposition $\mathbf{R} = \mathbf{V}\boldsymbol{\Lambda}\mathbf{V}^{-1}$ can have an infinity of solutions if the Jordan form $\mathbf{J}$ of $\mathbf{C}$ is non-diagonal. Second, even if $\mathbf{J}$ is diagonal, the complex scalar logarithm is non-unique, which is the case relevant for practical applications.

2.2.1. Modal decomposition of transient solution

A transient solution of the time-invariant Lyapunov–Floquet transformed system Eq. (18) is

$$\mathbf{z} = \mathrm{e}^{\mathbf{A}_\mathrm{L} t}\mathbf{z}(0) \tag{23}$$

where $\mathbf{z}(0) = \mathbf{L}^{-1}(0)\mathbf{x}(0)$ are the inverse transformed initial conditions. The transformed system matrix (19) can be Jordan decomposed as

$$\mathbf{A}_\mathrm{L} = \mathbf{V}_\mathrm{L}\boldsymbol{\Lambda}\mathbf{V}_\mathrm{L}^{-1} \tag{24}$$

where $\mathbf{V}_\mathrm{L} = \mathbf{L}^{-1}(0)\boldsymbol{\varphi}(0)\mathbf{V}$ and the Jordan form of $\mathbf{A}_\mathrm{L}$ is $\boldsymbol{\Lambda}$, because $\mathbf{A}_\mathrm{L}$ is a similarity transform of $\mathbf{R}$ (19). The transient solution (23) then becomes

$$\mathbf{z} = \mathbf{V}_\mathrm{L}\,\mathrm{e}^{\boldsymbol{\Lambda} t}\mathbf{V}_\mathrm{L}^{-1}\mathbf{z}(0) \tag{25}$$

Note the similarity between this expression and (8). The transient solution (25) can be modally decomposed and written in the original coordinates using (16) as

$$\mathbf{x} = \mathbf{U}(t)\,\mathrm{e}^{\boldsymbol{\Lambda} t}\mathbf{q}(0) \tag{26}$$

where the initial modal coordinates are

$$\mathbf{q}(0) = \mathbf{V}_\mathrm{L}^{-1}\mathbf{L}^{-1}(0)\mathbf{x}(0) = \mathbf{V}^{-1}\boldsymbol{\varphi}^{-1}(0)\mathbf{x}(0) \tag{27}$$

and the periodic mode shape matrix is

$$\mathbf{U}(t) = \mathbf{L}(t)\mathbf{V}_\mathrm{L} = \mathbf{L}(t)\mathbf{L}^{-1}(0)\boldsymbol{\varphi}(0)\mathbf{V} \tag{28}$$

The periodicity of $\mathbf{U}$ follows from the periodicity of $\mathbf{L}$.

The matrix $\mathbf{R}$ defined by (21) from the monodromy matrix $\mathbf{C}$ is still undetermined due to the indeterminacy of the matrix logarithm in (22). However, when $\mathbf{J}$ (the Jordan form of $\mathbf{C}$) is diagonal, then $\boldsymbol{\Lambda}$ (the Jordan form of $\mathbf{R}$) will also be diagonal with the elements

$$\lambda_k = \frac{1}{T}\ln(\rho_k) \tag{29}$$

which are called the *characteristic exponents* of the monodromy matrix $\mathbf{C}$, and the similarity transformation matrix $\mathbf{P}$ that brings $\mathbf{C}$ to its Jordan form $\mathbf{J}$ will also bring $\mathbf{R}$ to its Jordan form $\boldsymbol{\Lambda}$, i.e. $\mathbf{V} = \mathbf{P}$. Furthermore, the diagonal property of $\boldsymbol{\Lambda}$ shows that the modal decomposition (26) can be written as

$$\mathbf{x} = \sum_{k=1}^{N} \mathbf{u}_k(t)\,\mathrm{e}^{\lambda_k t} q_k(0) \tag{30}$$

where $\mathbf{u}_k(t) = \mathbf{L}(t)\mathbf{L}^{-1}(0)\boldsymbol{\varphi}(0)\mathbf{v}_k$ is a periodic mode shape of mode number k in the original coordinates and $q_k(0)$ is its modal content in the initial condition.

The characteristic exponents (29) are given by the complex logarithm

$$\lambda_k = \sigma_k + \mathrm{i}\omega_k = \frac{1}{T}\ln(|\rho_k|) + \mathrm{i}\,\frac{1}{T}(\arg(\rho_k) + j_k 2\pi), \quad j_k \in \mathbb{Z} \tag{31}$$

where σ_k and ω_k are the real and imaginary parts of λ_k, respectively. The integers j_k in the imaginary parts are undetermined for each mode, i.e. the modal frequencies ω_k are not determined uniquely. A physical explanation to this indeterminacy is that frequencies depend on the observer's frame of reference, which is defined by a Lyapunov–Floquet transformation that is non-unique due to its dependency on $\mathbf{R}$ (16). The frequency indeterminacy is now resolved by *defining modal frequencies as those frequencies observed in frequency responses measured in the inertial frame of reference*.

2.2.2. Resolving the indeterminacy of the modal frequencies

Principal Floquet exponents $\lambda_{\mathrm{p},k} = \sigma_k + \mathrm{i}\omega_{p,k}$ are defined by the modal damping σ_k and principal frequencies $\omega_{p,k}$ which are given by

$$\sigma_k = \frac{1}{T}\ln(|\rho_k|)$$
$$\omega_{p,k} = \frac{1}{T}\arg(\rho_k), \quad \omega_{p,k} \in \left]-\frac{1}{2}\Omega;\frac{1}{2}\Omega\right] \tag{32}$$

where $\arg(\rho_k) \in]-\pi;\pi]$ is implied. The complex logarithm (31) shows that the modal frequency ω_k is undetermined to within an integer multiple of the rotor speed:

$$\omega_k = \omega_{p,k} + j_k\Omega \tag{33}$$

where the indeterminacy for mode number k is denoted by the integer j_k. The transient response (30) to a pure excitation of mode k (obtainable by setting $q_k(0) = 1$ and all other initial modal components equal zero) can thereby be written as

$$\mathbf{x}_k(t) = \mathbf{u}_k(t)\,\mathrm{e}^{(\lambda_{\mathrm{p},k}+\mathrm{i}j_k\Omega)t} \tag{34}$$

where the periodic mode shape is given by (16) and (28) as

$$\begin{aligned}\mathbf{u}_k(t) &= \mathbf{L}(t)\mathbf{L}^{-1}(0)\boldsymbol{\varphi}(0)\mathbf{v}_k\,\mathrm{e}^{-(\lambda_{\mathrm{p},k}+\mathrm{i}j_k\Omega)t}\\ &= \boldsymbol{\varphi}(t)\mathbf{v}_k\,\mathrm{e}^{-(\lambda_{\mathrm{p},k}+\mathrm{i}j_k\Omega)t} = \mathbf{u}_{p,k}(t)\,\mathrm{e}^{-\mathrm{i}j_k\Omega t}\end{aligned} \tag{35}$$

where $\mathbf{u}_{p,k}(t) = \boldsymbol{\varphi}(t)\mathbf{v}_k\,\mathrm{e}^{-\lambda_{\mathrm{p},k}t}$ is the *principal periodic mode shape*. Both the periodic mode shape $\mathbf{u}_k$ and the exponential term in the solution (34) depend on the chosen integers j_k. As the exponent has different signs in (34) and (35), the contributions from j_k cancel, and the same transient solution is obtained independent of the values of j_k. Hence, a modal frequency of mode number k can be defined freely within an integer multiple of Ω, a choice that also determines the observer's frame of reference. The observer of the modal frequencies (33) is placed in the inertial frame of reference, which makes the modal frequencies similar to those obtained by the Coleman transformation approach, where the periodic mode shapes are constant for the non-transformed inertial state variables. The objective of the suggested approach is therefore to make the inertial state variables in the periodic mode shapes constant, or as constant as possible.

The Fourier expansion of the principal periodic mode shape $\mathbf{u}_{p,k}(t)$ contains only harmonics of an integer multiple of Ω because $\mathbf{u}_{p,k}$ is T-periodic, and it can be expressed for state variable i as

$$u_{p,ik}(t) = \sum_{j=-\infty}^{\infty} \mathscr{U}_{p,j,ik}\,\mathrm{e}^{\mathrm{i}2\pi jt/T} = \sum_{j=-\infty}^{\infty} \mathscr{U}_{p,j,ik}\,\mathrm{e}^{\mathrm{i}j\Omega t} \tag{36}$$

where $\mathscr{U}_{p,j,ik}$ are the Fourier coefficients.[1] Using (35) and (36), the periodic mode shape corresponding to the modal frequency (33) can be written as

$$u_{ik}(t) = \sum_{j=-\infty}^{\infty} \mathscr{U}_{p,j,ik}\,\mathrm{e}^{\mathrm{i}(j-j_k)\Omega t} \tag{37}$$

By selecting the undetermined integer j_k for mode k as the index of the largest Fourier coefficient

$$j_k = \{j_k \in \mathbb{Z} | \mathscr{U}_{\mathrm{p}j_k,ik} \geqslant \mathscr{U}_{p,j,ik}\ \forall j \in \mathbb{Z}\} \tag{38}$$

the largest harmonic component in the periodic mode shape (37) is removed. Note the index i must correspond to a state variable in the inertial frame. In the case of an isotropic rotor, $\mathscr{U}_{p,j,ik}$ is non-zero only for one j_k, and u_{ik} is constant for inertial state variables. If the rotor has any anisotropy, internally or externally, then $\mathscr{U}_{p,j,ik}$ will have several non-zero components for inertial state variables, but the periodic mode shape $u_{ik}(t)$ is made as constant as possible using (38) to select j_k.

Johnson [16, p. 374] describes the above method in the following way: "One way to mechanize this choice of frequencies is to require that the mean value of the eigenvector have the largest magnitude; then the harmonic of largest magnitude in the eigenvector corresponding to the principal value of the eigenvalue gives the frequency $n2\pi/T$", where "eigenvector" refers to the periodic mode shape and n is j_k. The periodic mode shape has the largest mean value in time, when it is not oscillating. Johnson's statement is, however, in this context only valid when considering the inertial state variables, because the rotor state variable harmonics can be non-zero at other frequencies than the harmonics of the inertial state variables.

2.2.3. Similarity of Coleman and Lyapunov–Floquet transformations

For an isotropic rotor, the Lyapunov–Floquet transformed solution (23) must be identical to the Coleman transformed solution (7) when written in the original coordinates. Using the Jordan decomposed forms of the time-invariant system

[1] The frequency resolution of the Fourier series (36) must be exactly Ω implying that the Fast Fourier Transforms of the principal periodic mode shapes are computed from fundamental solutions obtained in 2^n time steps over the period T, where n is an integer.

matrices, this equality of the solutions becomes

$$\mathbf{B}(t)\mathbf{V}_{\mathrm{B}}\,\mathrm{e}^{\mathbf{\Lambda}_{\mathrm{B}}t}(\mathbf{B}(0)\mathbf{V}_{\mathrm{B}})^{-1}\mathbf{x}(0)=\mathbf{L}(t)\mathbf{V}_{\mathrm{L}}\,\mathrm{e}^{\mathbf{\Lambda}_{\mathrm{B}}t}(\mathbf{L}(0)\mathbf{V}_{\mathrm{L}})^{-1}\mathbf{x}(0) \tag{39}$$

where the Jordan forms $\mathbf{\Lambda}$ and $\mathbf{\Lambda}_{\mathrm{B}}$ are identical for the two approaches, because the modal frequencies in the Lyapunov–Floquet transformed solution are resolved in the inertial frame as in the Coleman transformation solution.

The initial values of the Lyapunov–Floquet transformation (16) $\mathbf{L}(0)$ can be chosen arbitrarily. Choosing $\mathbf{L}(0)=\mathbf{B}(0)$, the two similarity transformation matrices of the Jordan decomposed forms must be equal, $\mathbf{V}_{\mathrm{B}}=\mathbf{V}_{\mathrm{L}}$, to satisfy (39) at $t=0$, whereby also the transformations become equal, $\mathbf{L}(t)=\mathbf{B}(t)$, for all $t\in\mathbb{R}$.

Hence, the Coleman and Lyapunov–Floquet transformations are identical for an isotropic rotor when the Lyapunov–Floquet system matrix $\mathbf{R}$ is corrected for the initial conditions used in the fundamental solution (19), and when the Coleman transformation is used as initial condition for the Lyapunov–Floquet transformation. Thus, the Coleman transformation can be viewed as a special case of the Lyapunov–Floquet transformation which also renders systems with anisotropic rotors time-invariant.

3. Application to a wind turbine with hinged blades

A structural model of a wind turbine with a minimum degrees of freedom able to represent some of its fundamental structural dynamics is considered. Fig. 1 illustrates the turbine with three rigid flap-hinged blades and a rigid nacelle that can tilt and yaw on a rigid tower. The state vector is

$$\mathbf{x}=\{\theta_1,\dot\theta_1,\theta_2,\dot\theta_2,\theta_3,\dot\theta_3,\theta_x,\dot\theta_x,\theta_z,\dot\theta_z\}^{\mathrm{T}} \tag{40}$$

where θ_j is the flap-hinge angle of blade j, and θ_x and θ_z are the tilt and yaw angles of the nacelle, respectively.

The rotor is assumed to be mass balanced and gravity is neglected, whereby the model can be linearized around the steady-state equilibrium with constant rotor speed and zero deflection angles. In case of gravity, or a mass unbalance, this linearization is also valid if the deflections in the periodic equilibrium are not too large. The system equations are written in first-order form (1) with a periodic system matrix (55) in Appendix A. Dissipation is included in the model by viscous damping forces.

To investigate anisotropy, different values for the blade stiffnesses G_1, G_2, and G_3 can be applied. This type of anisotropy is chosen to avoid changing the steady-state equilibrium. Table 1 shows the model parameters chosen to represent a generic multi-MW turbine.

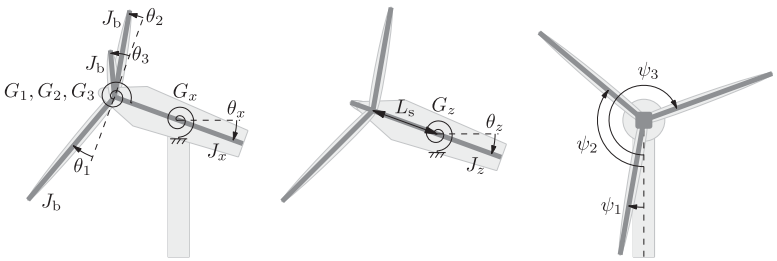

Fig. 1. A wind turbine with flapwise hinged rigid blades and a rigid nacelle able to tilt and yaw yielding five rotational degrees of freedom: θ_1, θ_2, θ_3, θ_x, and θ_z.

Table 1
Model parameters for a multi-MW generic wind turbine.

Blade moment of inertia about root	J_{b}	$4\times10^6\,\mathrm{kg\,m^2}$
Nacelle/tower tilt moment of inertia	J_x	$8\times10^6\,\mathrm{kg\,m^2}$
Nacelle/tower yaw moment of inertia	J_z	$6\times10^6\,\mathrm{kg\,m^2}$
Blade stiffness	G_{b}	$8\times10^7\,\mathrm{N\,m}$
Nacelle/tower tilt stiffness	G_x	$7\times10^8\,\mathrm{N\,m}$
Nacelle/tower yaw stiffness	G_z	$4\times10^8\,\mathrm{N\,m}$
Blade damping	c_{b}	$1\times10^5\,\mathrm{kg\,m^2\,s^{-1}}$
Nacelle/tower tilt damping	c_x	$1\times10^6\,\mathrm{kg\,m^2\,s^{-1}}$
Nacelle/tower yaw damping	c_z	$8\times10^5\,\mathrm{kg\,m^2\,s^{-1}}$
Blade mass	m_{b}	$12\times10^3\,\mathrm{kg}$
Distance from tower top to hub	L_{s}	4 m

3.1. Isotropic rotor

The case of an isotropic rotor, $G_1 = G_2 = G_3 = G_b$, is studied to show the similarity of the Coleman and Lyapunov–Floquet transformation approaches.

3.1.1. Coleman transformation approach

Eigenvalue analysis of the time-invariant system matrix (56) in Appendix A yields modal frequencies, damping, and eigenvectors in multi-blade coordinates. The state variables based on these coordinates are

$$\mathbf{z}_B = \{a_0, \tilde{a}_0, a_1, \tilde{a}_1, b_1, \tilde{b}_1, \theta_x, \dot{\theta}_x, \theta_z, \dot{\theta}_z\}^T \tag{41}$$

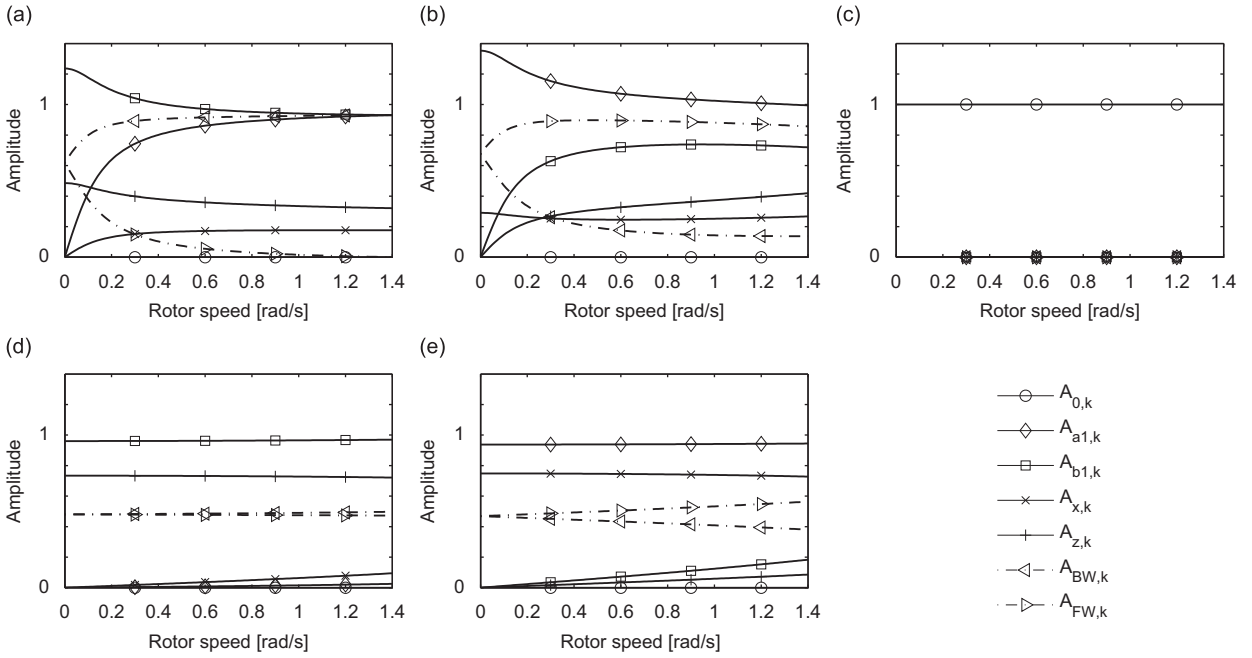

Fig. 2. Normalized modal amplitudes and whirling amplitudes versus rotor speed Ω. (a) First BW mode; (b) first FW mode; (c) symmetric mode; (d) second yaw mode; and (e) second tilt mode.

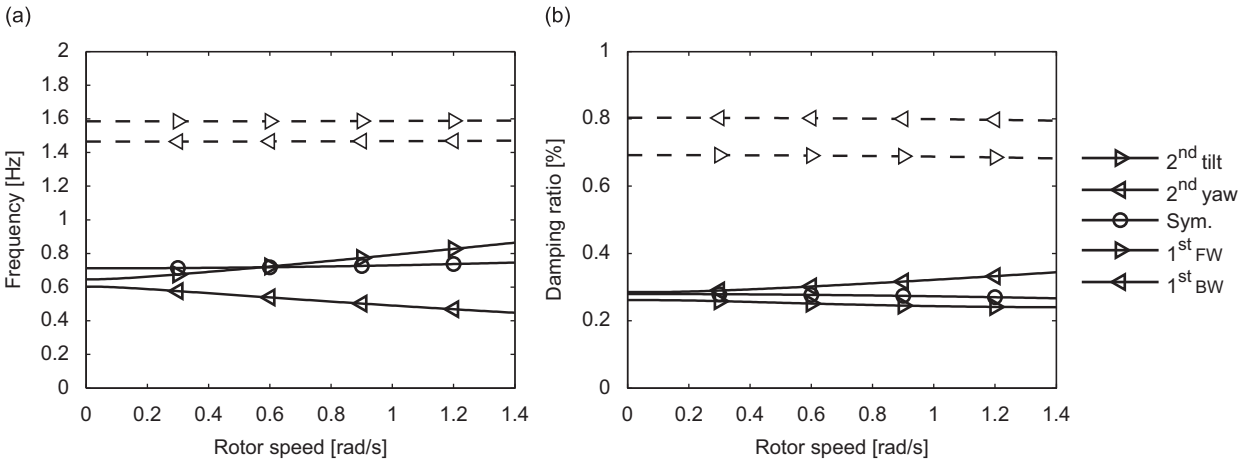

Fig. 3. (a) Campbell diagram with modal frequencies $f_k = \omega_k/2\pi$ versus rotor speed Ω. (b) Damping ratios (approx. $-\sigma_k/\omega_k$ for small damping values) versus rotor speed Ω.

where $\tilde{a}_0$, $\tilde{a}_1$, and $\tilde{b}_1$ are linear combinations of multi-blade positions and velocities (cf. Eq. (46) in Appendix A). The azimuth angle ψ_j for blade j is defined as zero for the blade pointing downwards (see Fig. 1), which means that the coordinate a_1 in (3) is rotor tilt motion, b_1 is yaw motion, and a_0 is the symmetric flap of the rotor.

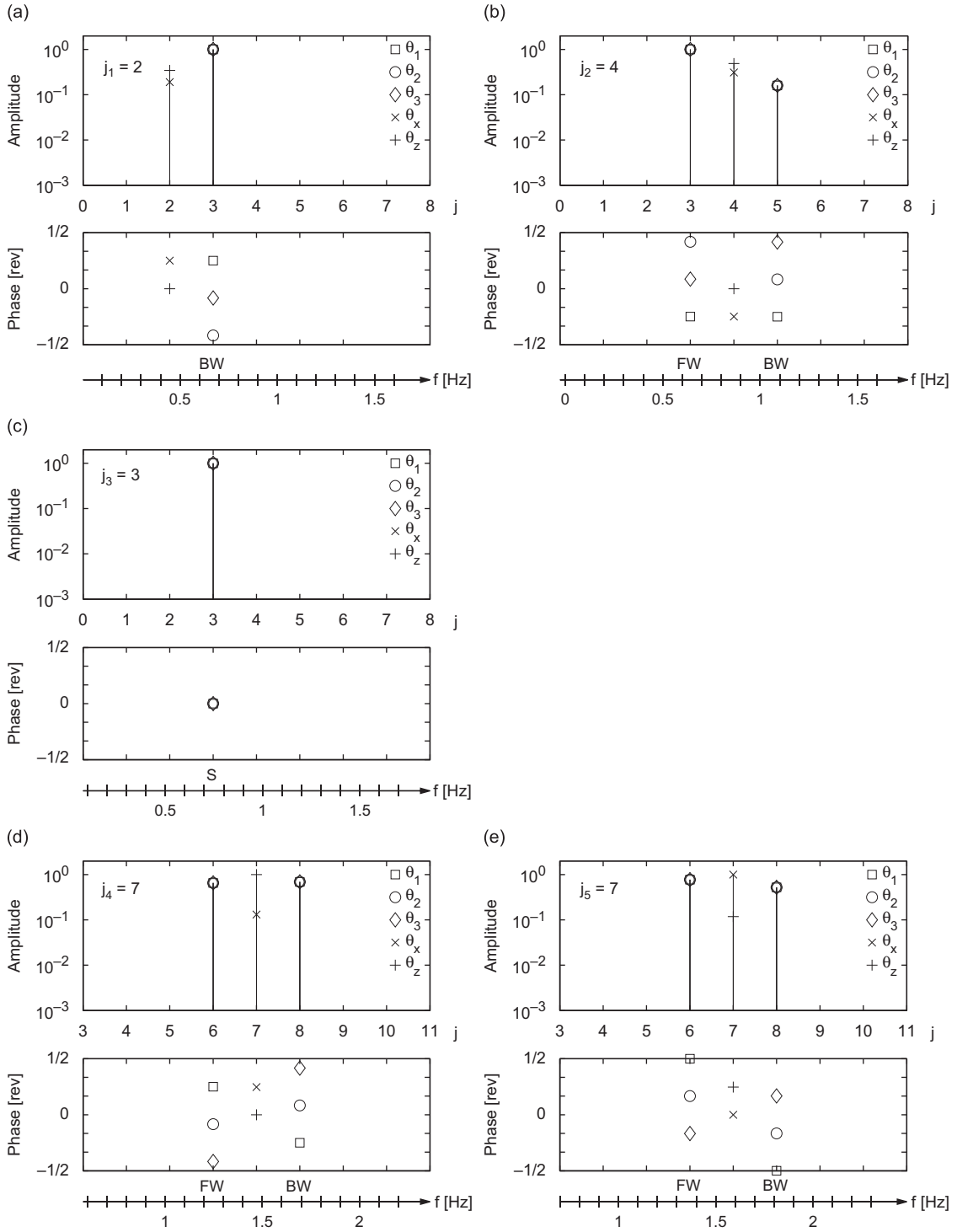

Fig. 4. Amplitudes (log. scale) and phases of harmonic components $\mathscr{U}_{p,j,ik}$ (36) in the principal periodic mode shape for the isotropic rotor at $\Omega = 1.4$ rad/s. The bottom scale shows the frequencies in the response measured in the inertial system as $(j - j_k)\Omega + \omega_k = j\Omega + \omega_{p,k}$ using (35). (a) First BW mode; (b) first FW mode; (c) symmetric mode; (d) second yaw mode; and (e) second tilt mode.

Fig. 2 shows the normalized modal amplitudes as function of rotor speed, where $A_{0,k}$, $A_{a_1,k}$, $A_{b_1,k}$, $A_{x,k}$, and $A_{y,k}$ are absolute values of the eigenvector components and $A_{\mathrm{BW},k}$ and $A_{\mathrm{FW},k}$ are obtained from (14) omitting subscripts $n = i = 1$. The tilt $A_{a_1,k}$ and yaw $A_{b_1,k}$ components represent rotor motion in the inertial frame, mutually exclusive to the whirling components $A_{\mathrm{BW},k}$ and $A_{\mathrm{FW},k}$ that represent rotor motion in the rotating frame. The first yaw mode (lowest frequency at standstill) develops into a mainly backward whirling mode for increasing rotor speed, whereas the first tilt mode develops into a mainly forward whirling mode. The second yaw and tilt modes with similar amounts of forward and backward whirling at all rotor speeds remain yaw and tilt modes. The symmetric mode has only the $A_{0,3}$ component and does not couple to the nacelle in this model with an isotropic rotor.

Fig. 3(a) shows the modal frequencies as function of rotor speed in a Campbell diagram. The frequency of the symmetric mode increases with the speed due to centrifugal stiffening, which derives from terms proportional to Ω^2 in the stiffness matrix (54c). The frequencies of the two lowest asymmetric modes split as they develop into backward and forward whirling modes, while the modal frequencies of the two highest asymmetric modes remain constant due to the small whirling amplitudes in these modes. Fig. 3(b) shows the damping ratios, which vary mainly due to the change in frequency.

3.1.2. Lyapunov–Floquet transformation approach

The periodic system equations (1) with (55) are integrated 10 times for linearly independent initial conditions $\boldsymbol{\varphi}(0) = \mathbf{I}$ to obtain the fundamental solution matrix (15) and monodromy matrix (20). Eigenvalue analysis of the monodromy matrix yields 10 distinct characteristic multipliers with linearly independent eigenvectors, whereby the system can be modally decomposed. The characteristic exponents (29) provide the principal frequencies $\omega_{p,k}$ in the interval $]-\Omega/2;\Omega/2]$ and damping σ_k using (32). The principal periodic mode shapes $\mathbf{u}_{p,k}$ are computed from (35) with $j_k = 0$.

Fig. 4(a) shows the amplitudes and phases of the Ω-harmonic components in the principal periodic mode shape of the first BW mode at the rated rotor speed $\Omega = 1.4\,\mathrm{rad/s}$. The modal frequency is determined from (38) using the dominating inertial component θ_z as $\omega_{\mathrm{p},1} + 2\Omega \approx 0.45\,\mathrm{Hz}$. The modal frequency of the first FW mode shape is similarly determined as $\omega_{\mathrm{p},2} + 4\Omega \approx 0.86\,\mathrm{Hz}$ from Fig. 4(b).

The direction of the rotor whirl can be determined from the phases of the individual blades. If the difference in phase between all blades is less than $\pi/3$, the harmonic is termed symmetric (S); otherwise it is termed backward whirling (BW) or forward whirling (FW) depending on the order of the phases of the individual blades (cf. Eq. (13)). The dominating rotor state variable harmonics in Figs. 4(a) and (b) thereby identify the first BW and first FW modes, respectively.

The phases in Fig. 4(c) show that the motion of the rotor state variables is symmetric, which means that they oscillate with the modal frequency. Thus, in the absence of any motion of the inertial state variables, the modal frequency is determined from the rotor component θ_1 as $\omega_{\mathrm{p},3} + 3\Omega \approx 0.75\,\mathrm{Hz}$.

The mode in Fig. 4(d) is termed the second yaw mode because θ_z is the most dominating inertial component, and because the BW and FW components are similar in magnitude, whereby the mode cannot be characterized as whirling. The modal frequency is determined from the θ_z component as $\omega_{\mathrm{p},4} + 7\Omega \approx 1.47\,\mathrm{Hz}$. Similarly, the mode in Fig. 4(e) is termed the second tilt mode from the dominating θ_x component and has modal frequency $\omega_{\mathrm{p},5} + 7\Omega \approx 1.59\,\mathrm{Hz}$.

The amplitudes of the Ω-harmonic components in the principal periodic mode shape are listed in Table 2. They are equal to the modal amplitudes obtained from the Coleman transformation approach shown in Fig. 2 for $\Omega = 1.4\,\mathrm{rad/s}$.

3.2. Anisotropic rotor

An anisotropy is applied to the blade stiffnesses as $G_1 = 1.1G_\mathrm{b}$ and $G_2 = G_3 = 0.95G_\mathrm{b}$ such that the mean stiffness is not changed. The modal frequencies determined from the Lyapunov–Floquet transformation approach change less than 0.5 percent compared to the isotropic case. Fig. 5(a) shows the amplitudes of the Ω-harmonic components in the principal periodic mode shape of the first BW mode. The mode shape now contains several Ω-harmonics, whereas there are at most three Ω-harmonics in the isotropic case. Similar results are obtained for the other asymmetric modes in Figs. 5(b, d, e).

Fig. 5(c) shows that the symmetric mode is not pure, i.e. there are whirling components in the mode shape. The stiffness anisotropy causes several Ω-harmonics in the symmetric mode shape for state variables in both the inertial and rotating

Table 2
For the isotropic rotor: modal frequencies and normalized amplitudes obtained from a Fourier transform of the periodic mode shape.

Mode	First BW	Sym.	First FW	Second tilt	Second yaw
f_k (Hz)	0.448	0.746	0.864	1.470	1.590
$A_{0,k}$ (f_k)	0.0000	1.0000	0.0000	0.0000	0.0000
$A_{\mathrm{BW},k}$ $(f_k + \Omega/2\pi)$	1.0000	0.0000	0.1605	0.6895	0.5228
$A_{\mathrm{FW},k}$ $(f_k - \Omega/2\pi)$	0.0002	0.0000	1.0000	0.6545	0.7748
$A_{x,k}$ (f_k)	0.1898	0.0000	0.3115	0.1310	1.0000
$A_{z,k}$ (f_k)	0.3449	0.0000	0.4888	1.0000	0.1181

Amplitudes $A_{0,k}$, $A_{\mathrm{BW},k}$, and $A_{\mathrm{FW},k}$ are obtained from θ_1 and $A_{x,k}$ and $A_{z,k}$ from θ_x and θ_z, respectively. In parentheses are noted the frequencies of the harmonic components, $\Omega/2\pi = 0.223\,\mathrm{Hz}$.

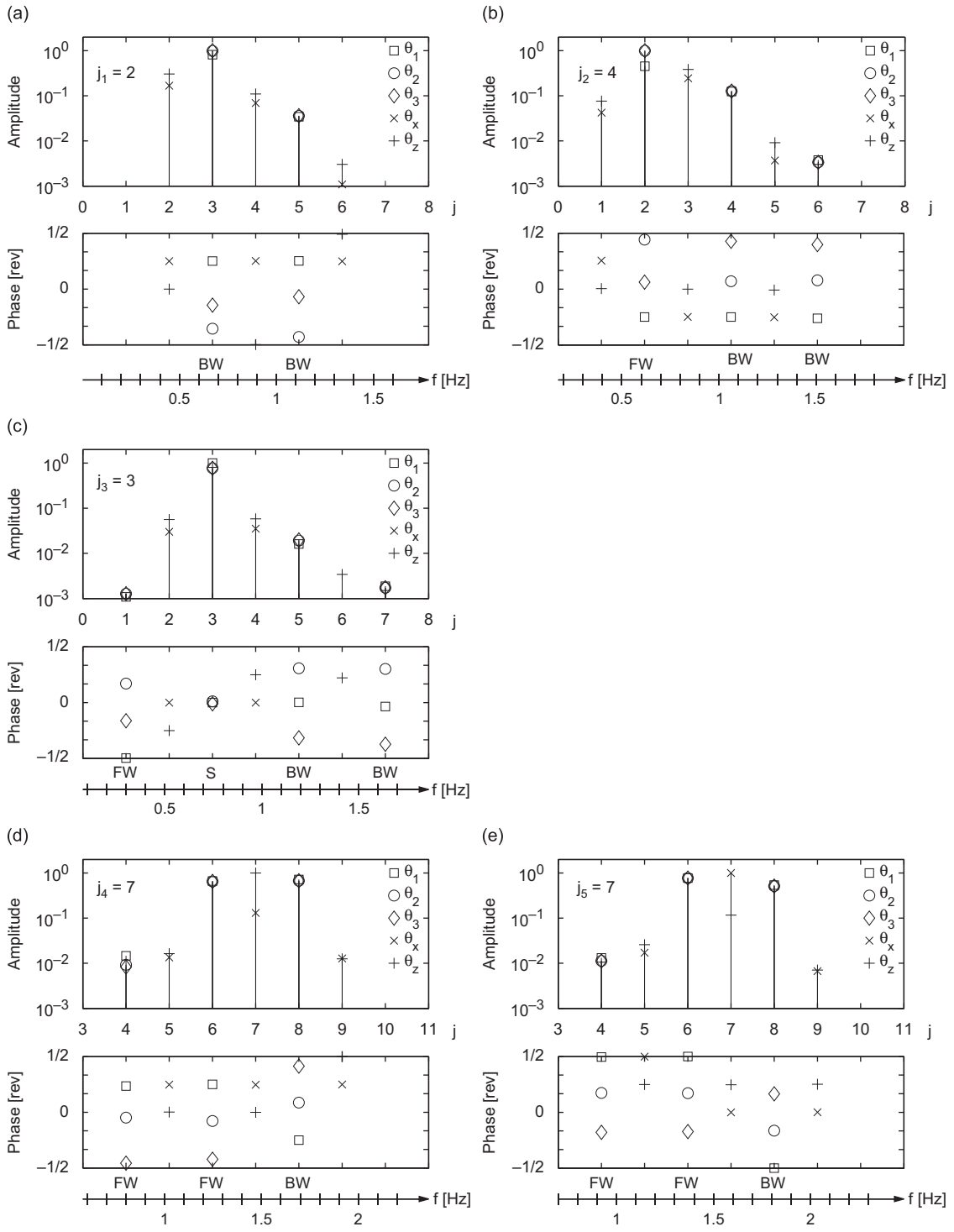

Fig. 5. Amplitudes (log. scale) and phases of harmonic components $\mathscr{U}_{p,j,ik}$ (36) in the principal periodic mode shape for the anisotropic rotor at $\Omega = 1.4\,\mathrm{rad/s}$. The bottom scale shows the frequencies in the response measured in the inertial system as $(j - j_k)\Omega + \omega_k = j\Omega + \omega_{p,k}$ using (35). (a) First BW mode; (b) first FW mode; (c) symmetric mode; (d) second yaw mode; and (e) second tilt mode.

frames, unlike the isotropic case involving only one harmonic in the rotor state variables. The symmetric mode has BW rotor components at even multiples of Ω above the symmetric rotor harmonic (the difference between the symmetric and the BW harmonics is an even number) and FW rotor components at even multiples of Ω below it.

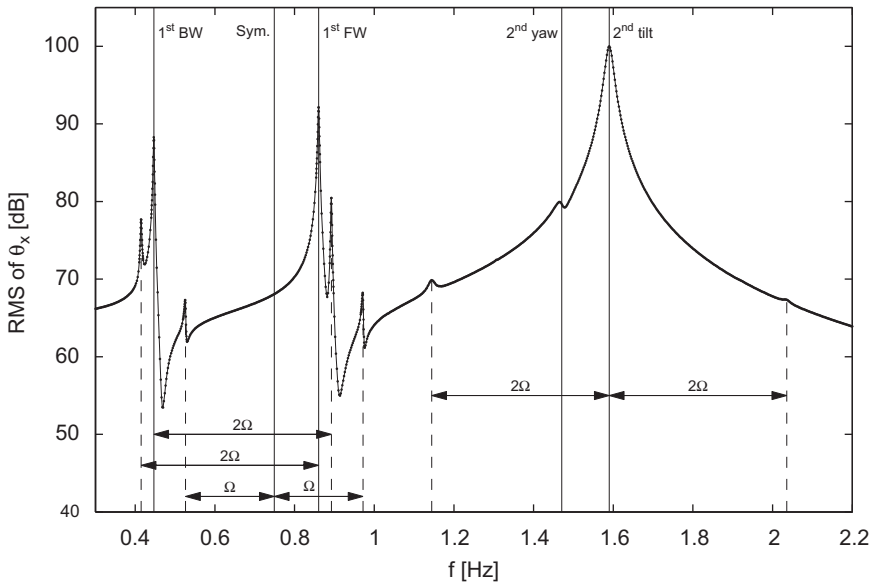

Fig. 6. RMS values of the steady-state nacelle tilt response θ_x (containing multiple harmonics) due to a harmonic excitation on the same degree of freedom for the anisotropic rotor and $\Omega = 1.4\,\mathrm{rad/s} = 0.223\,\mathrm{Hz}$.

The asymmetric mode shapes in Figs. 5(a, b, d, e) have BW and FW rotor components next to the dominating inertial component as in the isotropic case (cf. Eq. (13)). Additionally, the anisotropy creates BW rotor components at odd multiples of Ω above the dominating inertial component and FW rotor components at odd multiples of Ω below it. For all modes the inertial components appear between the whirling rotor components with an interval of 2Ω.

To study the effect of the additional harmonic components in the periodic mode shapes of the anisotropic rotor, the steady-state tilt response θ_x due to a harmonic excitation on θ_x is computed for a range of frequencies by a brute force approach using time integrations until a steady-state is reached for each excitation frequency. Steady state is here defined as the case where the frequency spectra of the response in two successive time intervals of 64 excitation periods are similar, with a maximum relative difference of 1 percent between the frequency components that have amplitudes larger than 0.1 percent of the maximum amplitude. These steady states may contain multiple harmonics, and the response is therefore represented by the rms value taken over the 64 excitation periods.

Fig. 6 shows peaks in the response at the modal frequencies denoted by the solid lines, except for the symmetric mode, due to the asymmetry of the excitation. The first smaller peak at $f_2 - 2\Omega = 0.41\,\mathrm{Hz}$ matches the harmonic at 2Ω below the dominating harmonic component of θ_x in the mode shape of the first FW mode in Fig. 5(b). Likewise, the peak at $f_1 + 2\Omega = 0.89\,\mathrm{Hz}$ is 2Ω above the frequency of the dominating harmonic of θ_x in the first BW mode shape in Fig. 5(a). The peaks around the symmetric modal frequency at $f_3 - \Omega = 0.53\,\mathrm{Hz}$ and $f_3 + \Omega = 0.97\,\mathrm{Hz}$ correspond respectively to the harmonics of θ_x at $\mp\Omega$ around the dominating rotor harmonic in Fig. 5(c). The two peaks at $f_5 - 2\Omega = 1.14\,\mathrm{Hz}$ and $f_5 + 2\Omega = 2.04\,\mathrm{Hz}$ correspond respectively to the harmonics of θ_x at $\mp 2\Omega$ around the dominating harmonic of θ_x in the second tilt mode shape in Fig. 5(d). The response has a small peak at the second yaw modal frequency because θ_x motion is involved only slightly in this mode, as seen by the amplitude of θ_x being much smaller than that of θ_z in the dominating harmonic in Fig. 5(e). This forced response analysis confirms the validity of predicting important aspects of the response by using the modal frequencies and periodic mode shapes. The obtained insight about Ω-harmonics in the periodic mode shape and their relation to the modal characteristics (symmetric or whirling rotor modes) can be used to understand frequency spectra and identify modes in measured or simulated time series of design determining loads.

4. Conclusion

In this paper, two methods for modally analyzing structures with bladed rotors are considered: the Coleman transformation approach and the Lyapunov–Floquet (L–F) transformation approach. The Coleman transformation is a special case of the L–F transformation for an isotropic rotor. The Coleman approach transforms rotor state variables into the inertial frame of reference and makes the system equations of structures with an isotropic rotor time-invariant, enabling eigenvalue analysis. The L–F approach is applicable to any periodic system but introduces an indeterminacy on the system frequencies and the transformation yielding a time-invariant system. Based on the similarity of the Coleman and the L–F approaches, the modal frequencies in the L–F approach are chosen such that the periodic mode shapes become as constant as possible for inertial state variables. In the example with a three-bladed wind turbine with an isotropic rotor the modal frequencies obtained using both approaches are identical. When introducing a rotor anisotropy to the blade stiffnesses,

meaningful modal frequencies are still obtained. However, state variables in the periodic mode shape, both in the rotor and in the inertial frame, now contain multiple harmonics that lead to multiple resonance frequencies for a single mode.

Acknowledgment

This work has been partially supported by the Danish Ministry of Science, Technology and Innovation through the Industrial PhD programme.

Appendix A

The equations of motion of a structure with a bladed rotor linearized about a steady state can be written in second-order form as

$$\mathbf{M}(t)\ddot{\mathbf{y}} + \mathbf{C}(t)\dot{\mathbf{y}} + \mathbf{K}(t)\mathbf{y} = \mathbf{0} \tag{42}$$

where $\mathbf{y}$ contains the generalized coordinates of the system, and the matrices $\mathbf{M}$, $\mathbf{C}$, and $\mathbf{K}$ are the periodic mass, gyroscopic/damping, and stiffness matrices, respectively. For an isotropic rotor, these periodic matrices of the second-order equations can all be written in a generic form as

$$\mathbf{G}(t) = \begin{bmatrix} \mathbf{G}_\mathrm{b} & \mathbf{G}_{bb,1} & \mathbf{G}_{bb,2} & \cdots & \mathbf{G}_{bb,2} & \mathbf{G}_{bb,1} & \mathbf{G}_{bs,1}(t) \\ \mathbf{G}_{bb,1} & \mathbf{G}_\mathrm{b} & \mathbf{G}_{bb,1} & \cdots & \mathbf{G}_{bb,3} & \mathbf{G}_{bb,2} & \mathbf{G}_{bs,2}(t) \\ \mathbf{G}_{bb,2} & \mathbf{G}_{bb,1} & \mathbf{G}_\mathrm{b} & \cdots & \mathbf{G}_{bb,4} & \mathbf{G}_{bb,3} & \mathbf{G}_{bs,3}(t) \\ \vdots & \vdots & \vdots & \ddots & \vdots & \vdots & \vdots \\ \mathbf{G}_{bb,2} & \mathbf{G}_{bb,3} & \mathbf{G}_{bb,4} & \cdots & \mathbf{G}_\mathrm{b} & \mathbf{G}_{bb,1} & \mathbf{G}_{bs,B-1}(t) \\ \mathbf{G}_{bb,1} & \mathbf{G}_{bb,2} & \mathbf{G}_{bb,3} & \cdots & \mathbf{G}_{bb,1} & \mathbf{G}_\mathrm{b} & \mathbf{G}_{bs,B}(t) \\ \mathbf{G}_{sb,1}(t) & \mathbf{G}_{sb,2}(t) & \mathbf{G}_{sb,3}(t) & \cdots & \mathbf{G}_{sb,B-1} & \mathbf{G}_{sb,B} & \mathbf{G}_\mathrm{s} \end{bmatrix} \tag{43}$$

where $\mathbf{G}_\mathrm{b}$ and $\mathbf{G}_\mathrm{s}$ are constant matrices describing the internal forces in the individual blades and the support and

$$\begin{aligned} \mathbf{G}_{sb,i}(t) &= \mathbf{G}^\mathrm{c}_\mathrm{sb}\cos\psi_i + \mathbf{G}^\mathrm{s}_\mathrm{sb}\sin\psi_i \\ \mathbf{G}_{bs,i}(t) &= \mathbf{G}^\mathrm{c}_\mathrm{bs}\cos\psi_i + \mathbf{G}^\mathrm{s}_\mathrm{bs}\sin\psi_i \end{aligned} \tag{44}$$

where $\mathbf{G}^s_\mathrm{bs}$, $\mathbf{G}^c_\mathrm{bs}$, $\mathbf{G}^s_\mathrm{sb}$, and $\mathbf{G}^c_\mathrm{sb}$ are constant matrices describing the coupling forces between blades of the rotor and its support. The constant matrices $\mathbf{G}_{bb,i}$ describe the coupling forces between blades j and $j+i$.

A.1. Coleman transformation of first-order state space equations

The Coleman transformation of state variables (3) implies that the generalized coordinates and velocities are transformed as

$$\mathbf{y} = \mathbf{B}_2\mathbf{z}_2 \quad \text{and} \quad \dot{\mathbf{y}} = \mathbf{B}_2\tilde{\mathbf{z}}_2 \tag{45}$$

where the Coleman transformation matrix $\mathbf{B}_2$ is given by (3) with half sized $\mathbf{I}_{N_\mathrm{b}}$ and $\mathbf{I}_{N_\mathrm{s}}$ corresponding to the number of generalized coordinates, and not state variables. The vector $\tilde{\mathbf{z}}_2$ represents the Coleman transformed generalized velocities, which are related to the time derivatives of the Coleman transformed generalized coordinates as

$$\tilde{\mathbf{z}}_2 = \bar{\omega}_2\mathbf{z}_2 + \dot{\mathbf{z}}_2 \tag{46}$$

where $\bar{\omega}_2$ is the constant matrix relating the Coleman transformation matrix and its derivative [23] as

$$\dot{\mathbf{B}}_2(t) = \mathbf{B}_2(t)\bar{\omega}_2 \tag{47}$$

Using that $\ddot{\mathbf{y}} = \mathbf{B}_2\bar{\omega}_2\tilde{\mathbf{z}}_2 + \mathbf{B}_2\dot{\tilde{\mathbf{z}}}_2$ and (46), the Coleman transformation of the second-order equations (42) becomes

$$\mathbf{M}_\mathrm{B}\dot{\tilde{\mathbf{z}}}_2 + \mathbf{M}_\mathrm{B}\bar{\omega}_2\tilde{\mathbf{z}}_2 + \mathbf{C}_\mathrm{B}\tilde{\mathbf{z}}_2 + \mathbf{K}_\mathrm{B}\mathbf{z}_2 = \mathbf{0} \tag{48}$$

where $\mathbf{M}_\mathrm{B} = \mathbf{B}_2^{-1}\mathbf{M}\mathbf{B}_2$, $\mathbf{C}_\mathrm{B} = \mathbf{B}_2^{-1}\mathbf{C}\mathbf{B}_2$, and $\mathbf{K}_\mathrm{B} = \mathbf{B}_2^{-1}\mathbf{K}\mathbf{B}_2$ are Coleman transformed system matrices.

Eqs. (46) and (48) can be rewritten in matrix form as

$$\begin{Bmatrix} \dot{\mathbf{z}}_2 \\ \dot{\tilde{\mathbf{z}}}_2 \end{Bmatrix} = \begin{bmatrix} -\bar{\omega}_2 & \mathbf{I} \\ -\mathbf{M}_\mathrm{B}^{-1}\mathbf{K}_\mathrm{B} & -\mathbf{M}_\mathrm{B}^{-1}\mathbf{C}_\mathrm{B} - \bar{\omega}_2 \end{bmatrix} \begin{Bmatrix} \mathbf{z}_2 \\ \tilde{\mathbf{z}}_2 \end{Bmatrix} \tag{49}$$

where $\{\mathbf{z}_2^\mathrm{T}, \tilde{\mathbf{z}}_2^\mathrm{T}\}$ contains the multi-blade state variables and original support state variables.

To use the Coleman transformation given by (3), this multi-blade state vector and the original state vector containing the general coordinates $\mathbf{y}$ and velocities $\dot{\mathbf{y}}$ must be permuted as

$$\mathbf{x} = \mathbf{P}_{\mathrm{x}} \begin{Bmatrix} \mathbf{y} \\ \dot{\mathbf{y}} \end{Bmatrix}, \quad \mathbf{z} = \mathbf{P}_{\mathrm{x}} \begin{Bmatrix} \mathbf{z}_2 \\ \tilde{\mathbf{z}}_2 \end{Bmatrix} \tag{50}$$

where the permutation matrix $\mathbf{P}_{\mathrm{x}}$ orders the state variables in $\mathbf{x}$ as given by (2). The Coleman transformed system matrix (6) thereby becomes

$$\mathbf{A}_{\mathrm{B}} = \mathbf{P}_{\mathrm{x}} \begin{bmatrix} -\bar{\boldsymbol{\omega}}_2 & \mathbf{I} \\ -\mathbf{M}_{\mathrm{B}}^{-1}\mathbf{K}_{\mathrm{B}} & -\mathbf{M}_{\mathrm{B}}^{-1}\mathbf{C}_{\mathrm{B}} - \bar{\boldsymbol{\omega}}_2 \end{bmatrix} \mathbf{P}_{\mathrm{x}}^{\mathrm{T}} \tag{51}$$

where the matrices $\mathbf{M}_{\mathrm{B}}$, $\mathbf{C}_{\mathrm{B}}$, and $\mathbf{K}_{\mathrm{B}}$ are time-invariant for isotropic rotors, as seen by derivation of the Coleman transformation of the generic matrix (43) after substantial algebraic manipulation using the trigonometric addition formulas and identities for sums of harmonics of evenly spaced angles [16]:

$$\mathbf{G}_{\mathrm{B}} = \mathbf{B}_2^{-1}\mathbf{G}\mathbf{B}_2 = \begin{bmatrix} \mathbf{G}_{\mathrm{B},0} & \mathbf{0} & \mathbf{0} & \mathbf{0} & \mathbf{0} & \cdots & \mathbf{0} & \mathbf{0} & \mathbf{0} & \mathbf{0} \\ \mathbf{0} & \mathbf{G}_{\mathrm{B},1} & \mathbf{0} & \mathbf{0} & \mathbf{0} & \cdots & \mathbf{0} & \mathbf{0} & \mathbf{0} & \mathbf{G}_{\mathrm{bs}}^{c} \\ \mathbf{0} & \mathbf{0} & \mathbf{G}_{\mathrm{B},1} & \mathbf{0} & \mathbf{0} & \cdots & \mathbf{0} & \mathbf{0} & \mathbf{0} & \mathbf{G}_{\mathrm{bs}}^{s} \\ \mathbf{0} & \mathbf{0} & \mathbf{0} & \mathbf{G}_{\mathrm{B},2} & \mathbf{0} & \cdots & \mathbf{0} & \mathbf{0} & \mathbf{0} & \mathbf{0} \\ \mathbf{0} & \mathbf{0} & \mathbf{0} & \mathbf{0} & \mathbf{G}_{\mathrm{B},2} & \cdots & \mathbf{0} & \mathbf{0} & \mathbf{0} & \mathbf{0} \\ \vdots & \vdots & \vdots & \vdots & \vdots & \ddots & \vdots & \vdots & \vdots & \vdots \\ \mathbf{0} & \mathbf{0} & \mathbf{0} & \mathbf{0} & \mathbf{0} & \cdots & \mathbf{G}_{\mathrm{B},\tilde{B}} & \mathbf{0} & \mathbf{0} & \mathbf{0} \\ \mathbf{0} & \mathbf{0} & \mathbf{0} & \mathbf{0} & \mathbf{0} & \cdots & \mathbf{0} & \mathbf{G}_{\mathrm{B},\tilde{B}} & \mathbf{0} & \mathbf{0} \\ \mathbf{0} & \mathbf{0} & \mathbf{0} & \mathbf{0} & \mathbf{0} & \cdots & \mathbf{0} & \mathbf{0} & \mathbf{G}_{\mathrm{B},B/2} & \mathbf{0} \\ \mathbf{0} & \frac{B}{2}\mathbf{G}_{\mathrm{sb}}^{c} & \frac{B}{2}\mathbf{G}_{\mathrm{sb}}^{s} & \mathbf{0} & \mathbf{0} & \cdots & \mathbf{0} & \mathbf{0} & \mathbf{0} & \mathbf{G}_{\mathrm{s}} \end{bmatrix} \tag{52}$$

where the first B diagonal entries are defined by

$$\mathbf{G}_{\mathrm{B},i} = \mathbf{G}_{\mathrm{b}} + \sum_{n=1}^{\tilde{B}} 2\cos(2\pi i n/B)\mathbf{G}_{\mathrm{bb},n} + (-1)^i \mathbf{G}_{\mathrm{bb},B/2} \tag{53}$$

with $i = 0, 1, \ldots, \tilde{B}$ for B odd and $i = 0, 1, \ldots, \tilde{B}, B/2$ for B even.

A.2. Second-order system matrices of wind turbine with three flap-hinged blades

The mass matrix $\mathbf{M}$, gyroscopic/damping matrix $\mathbf{C}$, and stiffness matrix $\mathbf{K}$ for the wind turbine with flap-hinged blades in Fig. 1 are given by

$$\mathbf{M}(t) = \begin{bmatrix} J_{\mathrm{b}} & 0 & 0 & J_{\mathrm{b}}\cos\psi_1 & -J_{\mathrm{b}}\sin\psi_1 \\ 0 & J_{\mathrm{b}} & 0 & J_{\mathrm{b}}\cos\psi_2 & -J_{\mathrm{b}}\sin\psi_2 \\ 0 & 0 & J_{\mathrm{b}} & J_{\mathrm{b}}\cos\psi_3 & -J_{\mathrm{b}}\sin\psi_3 \\ J_{\mathrm{b}}\cos\psi_1 & J_{\mathrm{b}}\cos\psi_2 & J_{\mathrm{b}}\cos\psi_3 & J_x + \frac{3}{2}J_{\mathrm{b}} + J_0 & 0 \\ -J_{\mathrm{b}}\sin\psi_1 & -J_{\mathrm{b}}\sin\psi_2 & -J_{\mathrm{b}}\sin\psi_3 & 0 & J_z + \frac{3}{2}J_{\mathrm{b}} + J_0 \end{bmatrix} \tag{54a}$$

$$\mathbf{C}(t) = \begin{bmatrix} c_1 & 0 & 0 & -2\Omega J_{\mathrm{b}}\sin\psi_1 & -2\Omega J_{\mathrm{b}}\cos\psi_1 \\ 0 & c_2 & 0 & -2\Omega J_{\mathrm{b}}\sin\psi_2 & -2\Omega J_{\mathrm{b}}\cos\psi_2 \\ 0 & 0 & c_3 & -2\Omega J_{\mathrm{b}}\sin\psi_3 & -2\Omega J_{\mathrm{b}}\cos\psi_3 \\ 0 & 0 & 0 & c_x & 3\Omega J_{\mathrm{b}} \\ 0 & 0 & 0 & 3\Omega J_{\mathrm{b}} & c_z \end{bmatrix} \tag{54b}$$

$$\mathbf{K}(t) = \begin{bmatrix} G_1 + \Omega^2 J_{\mathrm{b}} & 0 & 0 & 0 & 0 \\ 0 & G_2 + \Omega^2 J_{\mathrm{b}} & 0 & 0 & 0 \\ 0 & 0 & G_3 + \Omega^2 J_{\mathrm{b}} & 0 & 0 \\ \Omega^2 J_{\mathrm{b}}\cos\psi_1 & \Omega^2 J_{\mathrm{b}}\cos\psi_2 & \Omega^2 J_{\mathrm{b}}\cos\psi_3 & G_x & 0 \\ -\Omega^2 J_{\mathrm{b}}\sin\psi_1 & -\Omega^2 J_{\mathrm{b}}\sin\psi_2 & -\Omega^2 J_{\mathrm{b}}\sin\psi_3 & 0 & G_z \end{bmatrix} \tag{54c}$$

where $J_0 = 3m_b L_s^2$ and $\psi_j = \Omega t + 2\pi(j-1)/3$. The periodic system matrix of the first-order equations (1) can be derived from

$$\mathbf{A}(t) = \mathbf{P}_x \begin{bmatrix} \mathbf{0} & \mathbf{I} \\ -\mathbf{M}^{-1}(t)\mathbf{K}(t) & -\mathbf{M}^{-1}(t)\mathbf{C}(t) \end{bmatrix} \mathbf{P}_x^T \tag{55}$$

Extracting the generic form of these system matrices, the Coleman transformed system matrix of the first-order equations can be derived from (51) and (52) as

$$\mathbf{A}_B = \begin{bmatrix} 0 & 1 & 0 & 0 \\ -\frac{G_b}{J_b} - \Omega^2 & -\frac{c_b}{J_b} & 0 & 0 \\ 0 & 0 & 0 & 1 \\ 0 & 0 & -\frac{G_b}{J_b} - \frac{3G_b}{2J_0+2J_x} - \Omega^2 & -c_b\left(\frac{3}{2J_0+2J_x} + \frac{1}{J_b}\right) \\ 0 & 0 & \Omega & 0 \\ 0 & 0 & 0 & \Omega \\ 0 & 0 & 0 & 0 \\ 0 & 0 & \frac{3G_b}{2J_0+2J_x} & \frac{3c_b}{2J_0+2J_x} \\ 0 & 0 & 0 & 0 \\ 0 & 0 & 0 & 0 \end{bmatrix}$$

$$\begin{bmatrix} 0 & 0 & 0 & 0 & 0 & 0 \\ 0 & 0 & 0 & 0 & 0 & 0 \\ -\Omega & 0 & 0 & 0 & 0 & 0 \\ 0 & -\Omega & \frac{G_x}{J_0+J_x} & \frac{c_x}{J_0+J_x} & 0 & 2\Omega \\ 0 & 1 & 0 & 0 & 0 & 0 \\ -\frac{G_b}{J_b} - \frac{3G_b}{2J_0+2J_z} - \Omega^2 & -c_b\left(\frac{3}{2J_0+2J_z} + \frac{1}{J_b}\right) & 0 & 2\Omega & -\frac{G_z}{J_0+J_z} & -\frac{c_z}{J_0+J_z} \\ 0 & 0 & 0 & 1 & 0 & 0 \\ 0 & 0 & -\frac{G_x}{J_0+J_x} & -\frac{c_x}{J_0+J_x} & 0 & 0 \\ 0 & 0 & 0 & 0 & 0 & 1 \\ -\frac{3G_b}{2J_0+2J_z} & -\frac{3c_b}{2J_0+2J_z} & 0 & 0 & -\frac{G_z}{J_0+J_z} & -\frac{c_z}{J_0+J_z} \end{bmatrix} \tag{56}$$

References

[1] R.P. Coleman, Theory of self-excited mechanical oscillations of hinged rotor blades, Technical Report NACA-WR-L-308, Langley Research Center, 1943, available from ⟨ntrs.nasa.gov⟩.

[2] A.M. Feingold, Theory of mechanical oscillations of rotors with two hinged blades, Technical Report NACA-WR-L-312, Langley Research Center, 1943, available from ⟨ntrs.nasa.gov⟩.

[3] R.P. Coleman, A.M. Feingold, Theory of ground vibrations of a two-blade helicopter rotor on anisotropic flexible supports, Technical Report NACA-TN-1184, Langley Research Center, 1947, available from ⟨ntrs.nasa.gov⟩.

[4] G. Floquet, Sur les équations différentielles linéaires à coefficients périodiques (on linear differential equations with periodic coefficients), *Annales scientifiques de l'École Normale Supérieure* 2 (12) (1883) 47–88.

[5] E.T. Whittaker, G.N. Watson, *A Course of Modern Analysis*, fourth ed., Cambridge University Press, London, 1927.

[6] L. Meirovitch, *Methods of Analytical Dynamics*, McGraw-Hill, New York, 1970.

[7] K.G. Lindh, P.W. Likins, Infinite determinant methods for stability analysis of periodic-coefficient differential equations, *AIAA Journal* 8 (4) (1970) 680–686.

[8] O.J. Lowis, The stability of rotor blade flapping motion at high tip speed ratios, Technical Report R. & M. No. 3544, Aeronautical Research Council, 1963, available from ⟨aerade.cranfield.ac.uk⟩.

[9] D.A. Peters, K.H. Hohenemser, Application of the Floquet transition matrix to problems of lifting rotor stability, *Journal of the American Helicopter Society* 16 (2) (1971) 25–33.

[10] P. Friedmann, C.E. Hammond, T.-H. Woo, Efficient numerical treatment of periodic systems with application to stability problems, *International Journal for Numerical Methods in Engineering* 11 (1977) 1117–1136.

[11] S.C. Sinha, R. Pandiyan, Analysis of quasilinear dynamical systems with periodic coefficients via Liapunov–Floquet transformation, *International Journal of Nonlinear Mechanics* 29 (5) (1994) 687–702.

[12] D.A. Peters, Fast Floquet theory and trim for multi-bladed rotorcraft, *Journal of the American Helicopter Society* 39 (4) (1994) 82–89.

[13] O.A. Bauchau, Y.G. Nikishkov, An implicit Floquet analysis for rotorcraft stability evaluation, *Journal of the American Helicopter Society* 46 (3) (2001) 200–209.
[14] G. Quaranta, P. Mantegazza, P. Masarati, Assessing the local stability of periodic motions for large multibody non-linear systems using proper orthogonal decomposition, *Journal of Sound and Vibration* 271 (2004) 1015–1038.
[15] O.A. Bauchau, J. Wang, Efficient and robust approaches to the stability analysis of large multibody systems, *Journal of Computational and Nonlinear Dynamics* 3 (2008).
[16] W. Johnson, *Helicopter Theory*, Princeton University Press, New Jersey, 1980.
[17] J. Dugundji, J.H. Wendell, Some analysis methods for rotating systems with periodic coefficients, *AIAA Journal* 21 (6) (1983) 890–897.
[18] J.H. Milgram, I. Chopra, Air resonance of hingeless rotor helicopters in trimmed forward flight, *Journal of the American Helicopter Society* 39 (4) (1994) 46–58.
[19] D. Lee, D.H. Hodges, M.J. Patil, Multi-flexible-body dynamic analysis of horizontal axis wind turbines, *Wind Energy* 5 (4) (2002) 281–300.
[20] J. Nagabhushanam, G.H. Gaonkar, Automatic identification of modal damping from Floquet analysis, *Journal of the American Helicopter Society* 40 (2) (1995) 39–42.
[21] V.A. Yakubovich, V.M. Starzhinskii, *Linear Differential Equations with Periodic Coefficients*, Wiley, New York, 1975.
[22] M.H. Hansen, Aeroelastic instability problems for wind turbines, *Wind Energy* 10 (2007) 551–577.
[23] M.H. Hansen, Improved modal dynamics of wind turbines to avoid stall-induced vibrations, *Wind Energy* 6 (2003) 179–195.
[24] A.H. Nayfeh, B. Balachandran, *Applied Nonlinear Dynamics*, Wiley, New York, 1995.
[25] A.M. Lyapunov, *The General Problem of Stability of Motion*, Taylor & Francis Ltd., London, 1992.
[26] E.A. Coddington, N. Levinson, *Theory of Ordinary Differential Equations*, McGraw-Hill, New York, 1955.
[27] P. Montagnier, C.C. Paige, R.J. Spiteri, Real Floquet factors of linear time-periodic systems, *System & Control Letters* 50 (2003) 251–262.
[28] F.R. Gantmacher, *The Theory of Matrices*, Vol. 1, Chelsea Publishing Company, New York, 1959.
[29] W.J. Culver, On the existence and uniqueness of the real logarithm of a matrix, *Proceedings of the American Mathematical Society* 17 (1966) 1146–1151.